Preparation, Characterization, and Biodegradability of Renewable Resource-Based Composites from Recycled Polylactide Bioplastic and Sisal Fibers

Chin-San Wu

Department of Chemical and Biochemical Engineering, Kao Yuan University, Kaohsiung County, Taiwan 82101, People's Republic of China

Received 11 October 2010; accepted 29 December 2010
DOI 10.1002/app.34223
Published online 27 July 2011 in Wiley Online Library (wileyonlinelibrary.com).

ABSTRACT: The biodegradability, morphology, and mechanical thermal properties of composite materials composed of polylactide (PLA) and sisal fibers (SFs) were evaluated. Composites containing acrylic acid-grafted PLA (PLA-*g*-AA/SF) exhibited noticeably superior mechanical properties because of greater compatibility between the two components. The dispersion of SF in the PLA-*g*-AA matrix was highly homogeneous as a result of ester formation and the consequent creation of branched and cross-linked macromolecules between the carboxyl groups of PLA-*g*-AA and hydroxyl groups in SF. Furthermore, with a lower melt temperature, the PLA-*g*-AA/SF composite is more readily processed than PLA/SF. Both composites were buried in soil to assess biodegradability. Both the PLA and the PLA-*g*-AA/SF composite films were eventually completely degraded, and severe disruption of film structure was observed after 6–10 weeks of incubation. Although the degree of weight loss after burial indicated that both materials were biodegradable even with high levels of SF, the higher water resistance of PLA-*g*-AA/SF films indicates that they were more biodegradable than those made of PLA. © 2011 Wiley Periodicals, Inc. J Appl Polym Sci 123: 347–355, 2012

Key words: composites; polylactide; biodegradability; sisal fiber

INTRODUCTION

The use of biodegradable polyesters from renewable and/or fossil sources has gained considerable attention in research and industry because of economic and environmental issues, such as waste management and carbon emissions in recent years. Polylactide (PLA) is a versatile new compostable polymer that is made from renewable resources such as corn, sugar beets, or rice by Cargill Dow's.[1] In contrast to conventional plastics, such as polypropylene and polyethylene, which require hundreds or even thousands of years to degrade, PLA can degrade into naturally occurring products in just a few years.[2] Hence, PLA is used for many applications, with its properties such as high degrees of transparency and biocompatibility and high melting point (155–175°C). Currently, there is an increasing interest in using PLA for biodegradable materials. Under a project of Cargill Dow Liability Co., the production of PLA will greatly increase to as much as employed more than 140,000 metric tons annually by 2002. Pragmatically, PLA has been used in composites with other polymers as a packaging material, planting cups, and disposable cups and has been proposed for use in agricultural applications, including plastic bags, greenhouse films, transparent films for wrapping food, and mulch films.[3–6] As with other aliphatic polyesters, the biocompatibility of PLA and its copolymers has led to several commercially successful applications.[7]

Unfortunately, PLA is relatively expensive. One way to reduce the cost of PLA composites is by blending them with natural biomaterials. Additionally, there is a continuing need to investigate more environmental-friendly and sustainable materials to replace existing materials as industry attempts to lessen the dependence on petroleum-based fuels and products. To this end, plant fibers that can increase the tensile strength of composites have been used recently as a means of reinforcing polymer matrices as a replacement for synthetic fibers. Sisal is an abundant natural fibers resource with excellent tensile strength that can improve the mechanical properties. Therefore, dried sisal fiber (SF) has been widely applied in thermoplastic composites. Moreover, though SFs ranging in length from millimeters to a centimeter and require a compatibilizing agent to wet the fibers,[8,9] the higher hydrophilicity of PLA results in a natural wetting of SF. Composites of

Correspondence to: C.-S. Wu (t50008@cc.kyu.edu.tw).
Contract grant sponsor: National Science Council (Taipei City, Taiwan, R.O.C.); contract grant number: NSC 99-2622-E-244-001-CC3

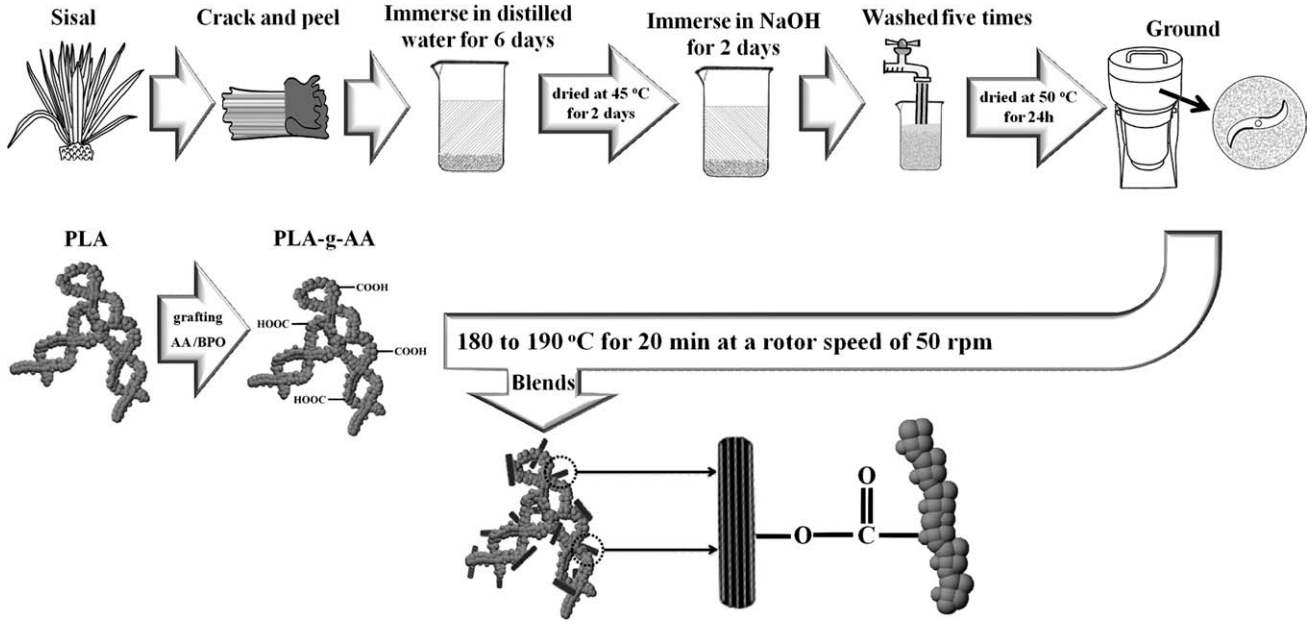

Scheme 1 Modification of PLA and SF and the preparation of composite materials.

PLA and SF thus offer advantages in both biocompatibility and cost.[10,11] Furthermore, composites of biodegradable polymers and natural fibers have demonstrated complete degradation in soil or compost without the emission of any toxic or noxious components and have thus received much attention.[12]

This report describes a systematic investigation of the mechanical properties and biodegradability of SF composites with PLA and acrylic acid (AA)-grafted PLA (PLA-*g*-AA). The composites were characterized using Fourier-transform infrared spectroscopy (FTIR) and ^{13}C nuclear magnetic resonance (NMR) to identify bulk structural changes induced by the AA moiety. Additionally, the effects of SF content on biodegradability were assessed for the PLA/SF and PLA-*g*-AA/SF composites. On the other way, the composites can be proved as a "green material" via biodegradation studies in soil environment. This result will serve as the norm of the composites in the future.

EXPERIMENTAL

Materials

Recycled polylactide (PLA) was purchased from Cargill Dow Corp. (Florham Park, NJ). Acrylic acid (AA), obtained from Sigma (St. Louis, MO), was purified before use by recrystallization from chloroform. Benzoyl peroxide (BPO; Sigma, Steinheim, Germany) was used as an initiator and was purified by dissolution in chloroform and reprecipitation in methanol. SF was obtained from Pingtung.

PLA-*g*-AA copolymer

Using BPO as the initiator, AA was grafted onto molten PLA under a nitrogen atmosphere at 190 ± 5°C with a mixer rotor speed of 60 rpm. A mixture of AA and BPO was added in four equal portions at 2-min intervals to the molten PLA to allow grafting to take place. Preliminary experiments showed that reaction equilibrium was attained in <10 h. Thus, reactions were allowed to progress for 10 h under stirring at a rotor speed of 60 rpm. The grafted product (~ 4 g) was then dissolved in 200 mL of refluxing xylene at 85 ± 2°C, and the hot solution was filtered through several layers of cheesecloth. The cheesecloth was washed with 600-mL acetone to remove the xylene-insoluble unreacted AA, and the product remaining on the cheesecloth was dried in a vacuum oven at 80°C for 24 h. Subsequently, the grafting percentage was determined using a titration method.[13] The titration showed a grafting percentage of about 6.86 wt %. BPO and AA loading were maintained at 0.3 and 10 wt %, respectively.

Sisal fiber processing

SF was extracted from crushed Taiwanese sisal. As shown in Scheme 1, purification consisted of immersing 50 g of ground and dried SF in 1000 mL of distilled water for 6 days to remove any water-soluble components. The product was then dried at 45°C for 2 days under vacuum. After drying, 1000 mL of NaOH (0.1*M*) was added to the SF. After 2 days, this suspension was vacuum-filtered. The product was washed five times and dried at 50°C

for 2 days under vacuum. The resulting light-yellow fibers were up to 6–8-cm long. The fibers were dried, ground, and sorted. After grinding, the fiber mixture consisted of a fine brown powder with dispersed pale-yellow single fibers, up to 150–500-μm long. The samples were passed through 60-mesh (0.246 mm) and 80-mesh (0.175 mm) sieves, air-dried for 2 days at 70–80°C, and vacuum-dried for at least 5 h at 105°C until the moisture content fell to 5 ± 1%.

Composite preparation

Prior to composite fabrication, SF samples were cleaned with acetone and dried in an oven at 105°C for 24 h. Composites were prepared in a "Plastograph" 200-Nm Mixer W50EHT with a blade rotor (Brabender, Dayton, OH). The composites were mixed between 180 and 190°C for 25 min at a rotor speed of 50 rpm. Samples were prepared with mass ratios of SF to PLA or to PLA-*g*-AA of 10/90, 20/80, 30/70, and 40/60. Residual AA in the PLA-*g*-AA reaction mixture was removed by acetone extraction prior to the preparation of PLA-*g*-AA/SF. After mixing, the composites were pressed into thin plates with a hot press and placed in a dryer for cooling. These thin plates were cut to standard sample dimensions for further characterization.

NMR/FTIR/DSC analyses

Solid-state ^{13}C-NMR spectra were acquired with an AMX-400 NMR spectrometer at 100 MHz under cross-polarization while spinning at the magic angle. Power decoupling conditions were set with a 90° pulse and a 4-s cycle time. Infrared spectra of the samples were obtained using a Bio-Rad FTS-7PC FTIR spectrophotometer. The glass transition temperature (T_g), melt temperature (T_m), and heat of fusion (ΔH_f) were determined using a TA instrument 2010 calorimeter. DSC sample amounts ranged from 4 to 6 mg, while melting curves were recorded from a low of −30°C to a high of 250°C at a rate of 10°C/min.

Mechanical testing

An Instron mechanical tester (Model LLOYD, LR5K type) was used to measure the tensile strength and the elongation at break in accordance with ASTM D638. Test samples were prepared in a hydrolytic press at 180°C and conditioned at 50 ± 5% relative humidity for 24 h before making measurements. Measurements were made using a crosshead speed of 20 mm/min. Five measurements were performed for each sample, and the mean value was determined.

Composite morphology

A thin film of each composite was created with a hydrolytic press and treated with hot water at 80°C for 24 h before being coated with gold. The surface morphology of these thin films was observed using a scanning electron microscope (SEM; Hitachi Microscopy Model *S*-1400, Tokyo, Japan).

Water absorption

Samples were prepared for water absorption measurements by cutting into 75-mm × 25-mm strips (150 ± 5 μm thick) in accordance with ASTM D570-81. The samples were dried in a vacuum oven at 50 ± 2°C for 8 h, cooled in a desiccator, and then immediately weighed to the nearest 0.001 g (W_c). Then, the samples were immersed in distilled water and maintained at 25 ± 2°C for a 6-week period. During this time, they were removed from the water at 7-day intervals, gently blotted with tissue paper to remove excess water from their surfaces, immediately weighed to the nearest 0.001 g (W_w), and returned to the water. Each W_w value was an average value obtained from three measurements. The percentage of weight increase due to water absorption (W_f) was calculated to the nearest 0.01% according to eq. (1):

$$\%W_f = ((W_w - W_c)/W_c) \times 100\%. \quad (1)$$

Biodegradation studies

Biodegradability of the samples was assessed by measuring the weight loss of the composites over time in a soil environment. Samples measuring 30 mm × 30 mm × 1 mm were weighed and buried in boxes of alluvial-type soil that had been obtained in May 2009 from farmland topsoil before planting. The soil was sifted to remove large clumps and plant debris. Procedures for soil burial were as described by Alvarez et al.[14] Soil was maintained at ~ 30% moisture by weight, and the samples were buried at a depth of 12−15 cm. A control box consisted of only samples and no soil. The buried samples were dug out after 2 weeks, washed in distilled water, dried in a vacuum oven at 50 ± 2°C for 2 days, and equilibrated in a desiccator for at least 1 day. The samples were then weighed before being returned to the soil.

RESULTS AND DISCUSSION

To investigate the variation of heat of fusion, melt temperatures, and glass transition temperature after replacing pure PLA with more compatible

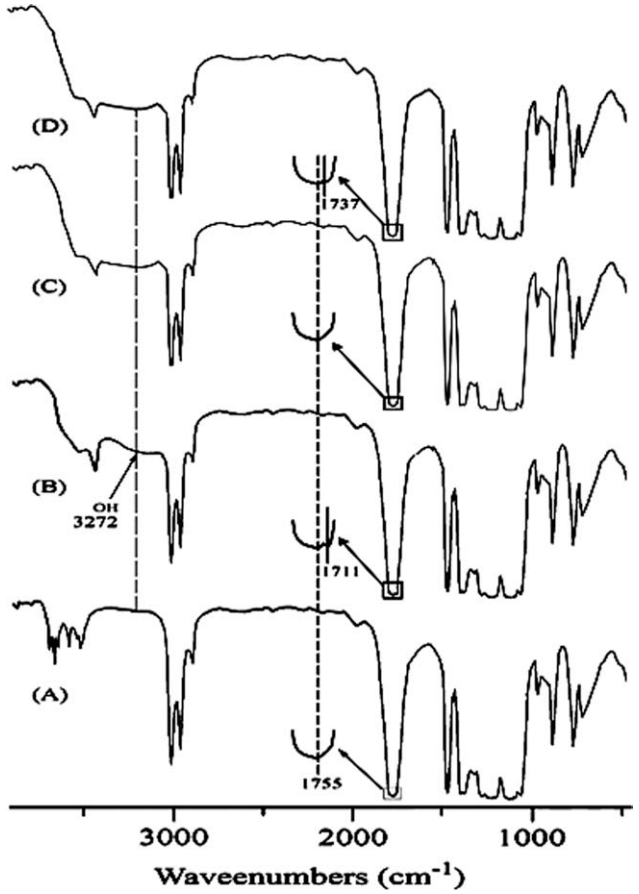

Figure 1 FTIR spectra for (A) PLA, (B) PLA-*g*-AA, (C) PLA/SF (20 wt %), and (D) PLA-*g*-AA/SF (20 wt %).

AA-grafted-PLA in SF-containing composites and prove the grafting of AA and the variation after mixing, the composites were characterized chemically using FTIR and NMR, thermally by DSC, and morphologically by SEM. On the other hand, the melt torque, mechanical properties, water absorption, and biodegradation were evaluated.

FTIR/NMR analyses

FTIR spectra of PLA, PLA-*g*-AA, PLA/SF, and PLA-*g*-AA/SF are shown in Figure 1. The characteristic peaks of PLA at 1700−1760 and 500−1500 cm^{-1} were observed in both neat PLA and in PLA-*g*-AA.[15] An additional peak at 1711 cm^{-1}, assigned to —C=O, and a broad O—H stretching transition at 3272 cm^{-1} were observed in the modified PLA. The shoulder near 1711 cm^{-1} was attributed to free acid in the modified polymer. This pattern of distinctive peaks indicated successful grafting of AA onto PLA. Similar results have been reported previously.[16] The peak assigned to the O—H stretching vibration at 3200−3700 cm^{-1} intensified in the PLA/SF (20 wt %) composite [Fig. 1(C)] because of contributions from the —OH group of SF. The FTIR spectrum of the PLA-*g*-AA/SF (20 wt %) composite in Figure 1(D) revealed a peak at 1737 cm^{-1} that was not present in the FTIR spectrum of the PLA/SF (20 wt %) composite. This peak was assigned to the ester carbonyl stretching vibration of the copolymer. Shah et al.[17] also reported an absorption peak at 1735 cm^{-1} for this ester carbonyl group. These data suggest the formation of branched and crosslinked macromolecules in the PLA-*g*-AA/SF composite by a covalent reaction of the AA carboxyl groups in PLA-*g*-AA with the hydroxyl groups of SF.

This hypothesis was confirmed by a comparison of the ^{13}C-NMR spectra of PLA and PLA-*g*-AA in Figure 2(A,B), respectively. There are three peaks corresponding to carbon atoms in the unmodified PLA (1 : δ = 16.95 ppm; 2 : δ = 68.78 ppm; and 3 : δ = 169.16 ppm). A similar result had been reported by Breitenbach et al.[18] The ^{13}C-NMR spectrum of PLA-*g*-AA showed additional peaks (4 : δ = 42.56 ppm; 5 : δ = 35.99 ppm; and 6 : —C=O δ = 174.98

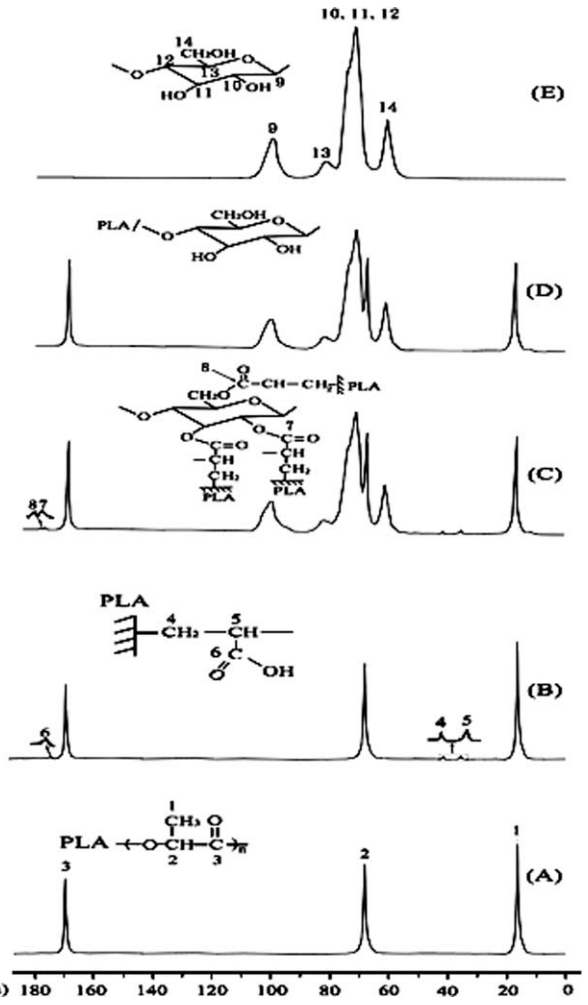

Figure 2 Solid-state ^{13}C-NMR spectra for (A) PLA, (B) PLA-*g*-AA, (C) PLA/SF (20 wt %), (D) PLA-*g*-AA/SF (20 wt %), and (E) SF.

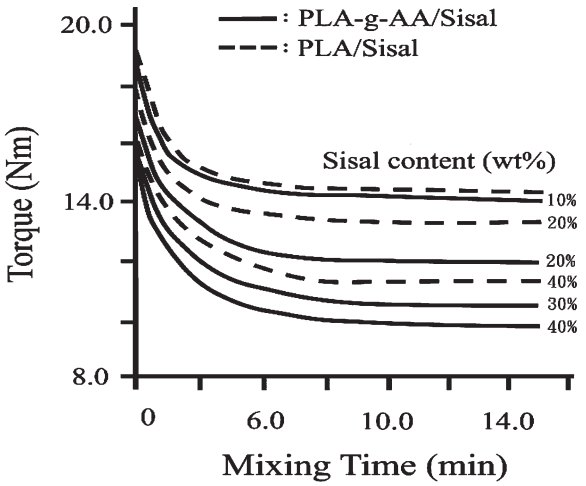

Figure 3 Torque values are plotted as a function of mixing time for PLA/SF and PLA-*g*-AA/SF composites with various SF content.

ppm), confirming that AA was covalently grafted onto PLA.

The solid-state ^{13}C-NMR spectra of PLA-*g*-AA/SF (20 wt %), PLA/SF (20 wt %), and SF are shown in Figure 2(C–E). The spectra are similar to those reported by Martins et al.[19] Relative to unmodified PLA, additional peaks were observed in the spectra of composites containing PLA-*g*-AA. These additional peaks were located at $\delta = 42.56$ ppm (4) and $\delta = 35.99$ ppm (5). These same features were observed in previous studies[16] and indicate grafting of AA onto PLA. However, the peak at $\delta = 174.98$ ppm (—C=O) (6) [Fig. 2(B)], which is also typical for AA grafted onto PLA, was absent in the solid-state spectrum of PLA-*g*-AA/SF (20 wt %). This is likely a result of an additional condensation reaction between the carboxyl group of AA and the —OH group of SF that caused the peak at $\delta = 174.98$ ppm to split into two signals of carbonyl groups in ester bonds ($\delta = 176.66$ and 177.92 ppm). This additional reaction converted the fully acylated groups in the original SF to esters [represented by peaks 7 and 8 in Fig. 2(C)] and did not occur between PLA and SF, as indicated by the absence of corresponding peaks in the FTIR spectrum of PLA/SF (20 wt %) in Figure 2(D). The formation of ester groups significantly affects the thermal and biodegradation properties of PLA-*g*-AA/SF and is discussed in greater detail in the following sections.

Torque measurements during mixing

The effects of SF content and mixing time on the melt torque of PLA/SF and PLA-*g*-AA/SF composites are shown in Figure 3. During the measurement, PLA or PLA-*g*-AA was first melted at 180–190°C. SF was then gradually added into the melt. Torque values decreased with increasing SF content and mixing time, approaching a stable value when the mixture was sufficiently mixed after 8 min. The final torque values decreased with increasing SF content, because the melt viscosity of SF was lower than that of PLA or PLA-*g*-AA. Thus, the melt viscosity of the entire blend was reduced. Additionally, melt torque values of the PLA-*g*-AA/SF composites were significantly lower than those of the PLA/SF composites at the same SF content. According to Wu,[20] this lowered melt viscosity was due to the formation of ester carbonyl groups (as discussed earlier), which led to conformational changes in the starch molecule.

Differential scanning calorimetry

The heats of fusion (ΔH_f) and melt temperatures (T_m) of both PLA/SF and PLA-*g*-AA/SF composites with various SF content were determined by measuring DSC heating thermograms (Table I). For both composites, T_m decreased with increasing SF content. This may be due to SF-induced expansion of PLA or PLA-*g*-AA, which produces a slack polymer structure and a reduced T_m. At the same SF content, the PLA/SF composites had a higher T_m than the PLA-*g*-AA/SF composites. This result is consistent with the corresponding torque measurements in Table I. The lower melt viscosity indicates that PLA-*g*-AA/SF is more readily processed than PLA/SF. The glass transition temperature (T_g) increased with increasing SF content for both PLA/SF and PLA-*g*-AA/SF composites. This increase was likely a result of decreasing space available for molecular motion. T_g values were higher for the PLA-*g*-AA composite by between 0.5 and 4.5°C, suggesting that the grafting of carboxyl groups to the PLA further restricted molecular motion.

The ΔH_f of neat PLA was 35.3 J/g, whereas that of PLA-*g*-AA was 32.9 J/g (Table I). The lower ΔH_f of PLA-*g*-AA was likely due to the disruption of regularity in chain structure and increased spacing between chains as a result of the grafted branches. The values of ΔH_f in PLA-*g*-AA/SF were $\sim$ 2–10 J/g

TABLE I
Effect of SF Content on the Thermal Properties of PLA/SF and PLA-*g*-AA/SF Composites

	PLA/SF			PLA-*g*-AA/SF		
SF (wt %)	T_g (°C)	T_m (°C)	ΔH_f (J/g)	T_g (°C)	T_m (°C)	ΔH_f (J/g)
0	57.1	158.5	35.3	56.5	158.1	32.9
10	57.9	155.9	27.2	60.8	155.1	31.6
20	58.8	153.8	24.1	62.9	151.8	31.1
30	59.6	153.1	22.2	64.1	151.5	30.5
40	60.2	152.9	20.1	64.7	151.3	30.1

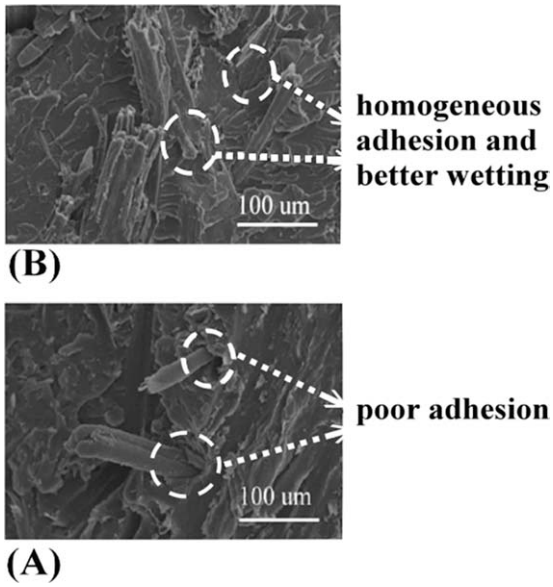

Figure 4 SEM photomicrographs show the distribution and adhesion of SF in (A) PLA/SF (20 wt %) and (B) PLA-*g*-AA/SF (20 wt %) composites.

higher than those of PLA/SF. These higher ΔH_f values were likely due to the formation of ester carbonyl groups as discussed earlier.

ΔH_f may be used as an indicator of composite crystallinity. Although ΔH_f of both the PLA/SF and PLA-*g*-AA/SF composites decreased with increasing SF (Table I), the extent of the decrease was significantly greater in PLA/SF, indicating a lower degree of crystallinity. These results are similar to those obtained with composites of PLA and other natural fibers.[21] The marked decrease in the crystallinity of PLA/SF was most likely due to hindered motion of the PLA polymer segments as a result of the presence of SF in the composite matrix. This can be considered a steric effect wherein the hydrophilic nature of SF led to poor adhesion with the more hydrophobic PLA matrix.[22]

Composite morphology

In most composite materials, effective wetting and uniform dispersion of all components in a given matrix and strong interfacial adhesion between the phases are required to obtain a composite with satisfactory mechanical properties. In the current study, SF may be thought of as a dispersed phase within a PLA or PLA-*g*-AA matrix. To evaluate the composite morphology, SEM was used to examine tensile fractures in the surfaces of PLA/SF (20 wt %) and PLA-*g*-AA/SF (20 wt %) samples. The SEM microphotograph of PLA/SF (20 wt %) in Figure 4(A) shows that the SF in this composite tended to agglomerate into bundles and was unevenly distributed in the matrix. This poor dispersion was due to the formation of hydrogen bonds among SF fibers and the disparate hydrophilicities of PLA and SF. Poor wetting in these composites was also noted [marked in Fig. 4(A)] because of the large differences in surface energy between the SF and the PLA matrix.[23] The PLA-*g*-AA/SF (20 wt %) photomicrograph in Figure 4(B) shows a more homogeneous dispersion and better wetting of SF in the PLA-*g*-AA matrix, indicated by the complete coverage of PLA-*g*-AA on the fiber and the removal of both materials when a fiber was pulled from the bulk. This improved interfacial adhesion was due to the similar hydrophilicity of the two components, allowing the formation of branched and crosslinked macromolecules and preventing hydrogen bonding between SF fibers.

Mechanical properties

Figure 5 shows the variation in tensile strength at break with SF content for PLA/SF and PLA-*g*-AA/SF composites. The tensile strength of neat PLA decreased when it was grafted with AA. For PLA/SF composites (dotted line in Fig. 5), tensile strength at break decreased markedly and continuously as the SF content increased. This is due to the poor dispersion of SF in the PLA matrix and demonstrates that incompatibility between the two polymers has a significant impact on the mechanical properties of the composite. The tensile strength of PLA-*g*-AA/SF (solid line in Fig. 5) is lower than that of PLA. Tensile strength increased at 10 wt % SF because of esterification between PLA-*g*-AA and SF. The tensile strength decreased at high levels of SF because of agglomeration and uneven distribution of residual SF, which was present due to the low grafting rate of 6.86%. Furthermore, it was found that the PLA-*g*-AA/SF composites not only gave larger values of

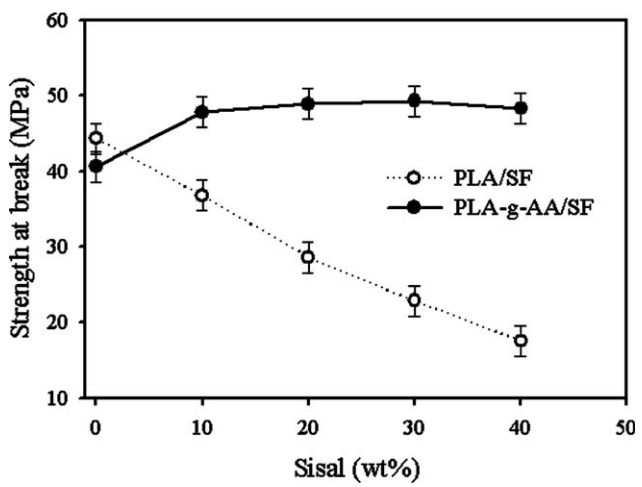

Figure 5 The effect of SF content on tensile strength at break is shown for PLA/SF and PLA-*g*-AA/SF composites.

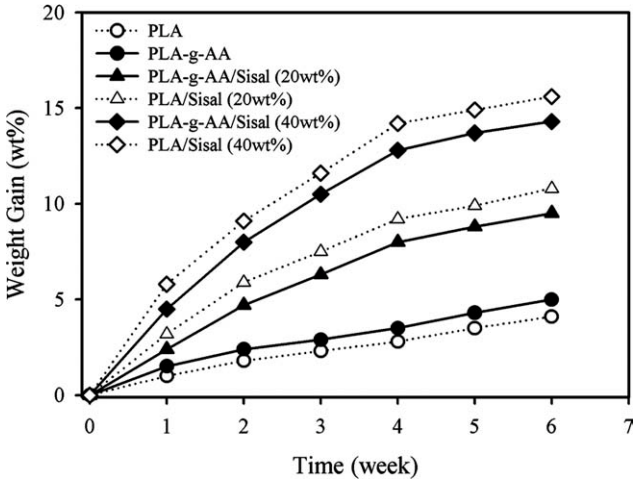

Figure 6 Percent weight gain due to the absorption of water for PLA/SF and PLA-*g*-AA/SF composites.

tensile strength than the PLA/SF composites but also yielded more stable tensile strengths when the SF content was above 20 wt %. This may be, in part, due to the more homogeneous dispersion resulting from the formation of branched or crosslinked macromolecules of SF in the PLA-*g*-AA matrix. Grafting of the AA onto PLA increased the tensile strength of the SF composite.

Water absorption

At the same SF content, the PLA-*g*-AA/SF composites exhibited higher water resistance than the PLA/SF composites (Fig. 6). The water resistance of the PLA-*g*-AA/SF composites was moderate, and it is proposed that the interaction of AA-grafted PLA with SF increased the hydrophobicity of SF in these composites. For both PLA/SF and PLA-*g*-AA/SF, the percent water gain over the 6-week test period was greater with higher SF content. Because the polymer chain exists in a presumably random arrangement, the earlier result was probably due to increased difficulty in forming ordered chain configurations with higher amounts of SF and to the hydrophilic character of SF, which adheres weakly to the more hydrophobic PLA.

Biodegradation in soil

Changes in the morphology of both the PLA and PLA-*g*-AA/SF composites were noted as a function of the amount of time buried in soil. SEM photomicrographs taken after 2, 6, and 14 weeks illustrate the extent of morphological change (Fig. 7). PLA/SF [20 wt %; Fig. 7(F–H)] exhibited larger and deeper pits that appeared to be more randomly distributed

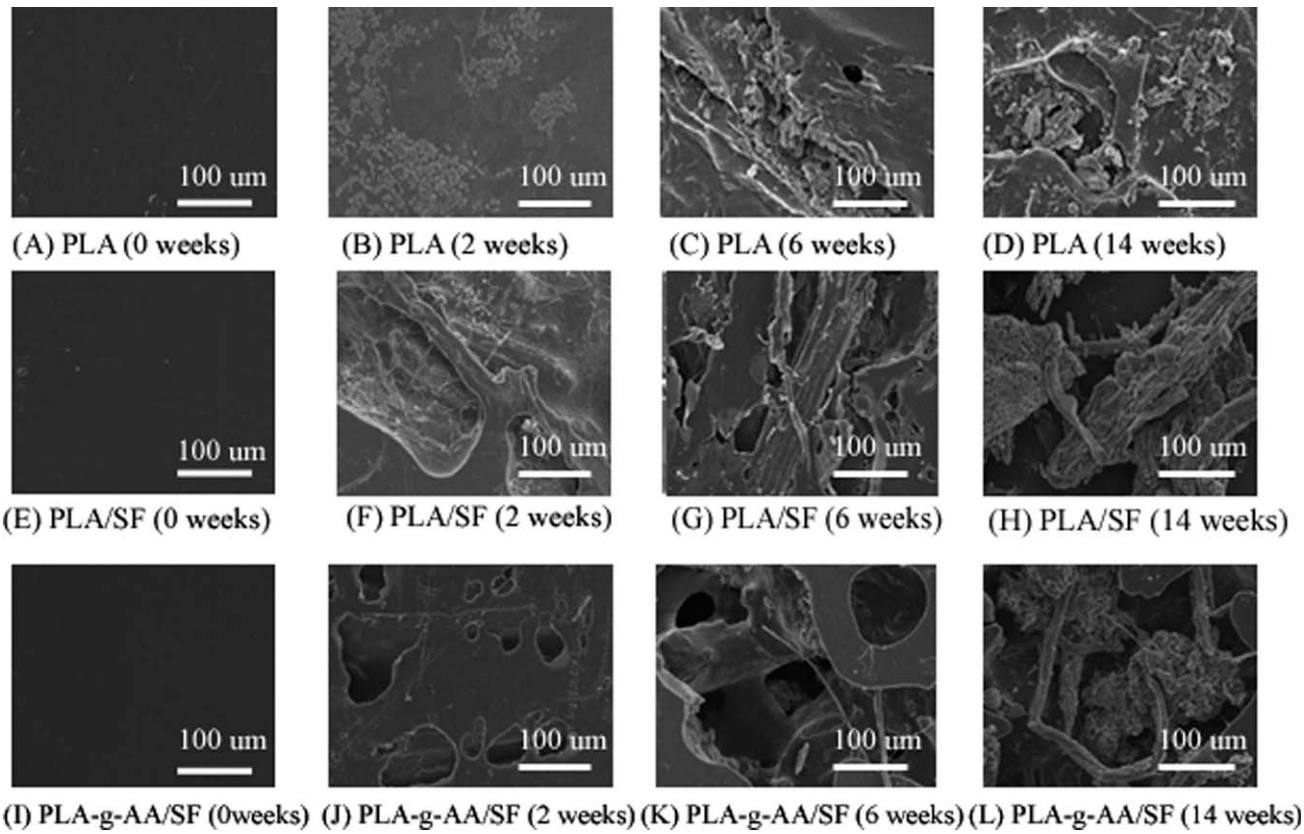

Figure 7 SEM micrographs show the morphology of PLA (A–D), PLA/SF (E–H), and PLA-*g*-AA/SF (I–L) films as a function of incubation time in soil.

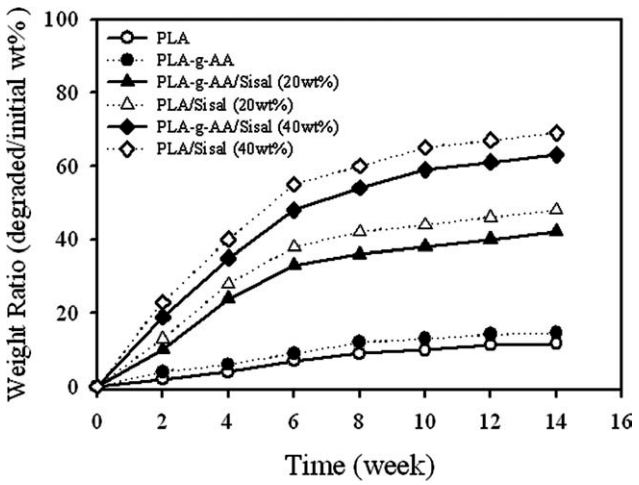

Figure 8 Weight loss percentages of PLA, PLA-*g*-AA, PLA/SF, and PLA-*g*-AA/SF are shown as a function of incubation time in soil.

relative to those in the PLA-*g*-AA/SF (20 wt %) composites [Fig. 7(J–L)]. These analyses also indicate that biodegradation of the SF phase in PLA/SF (20 wt %) increased with time, confirming the results presented in Figure 8.

After a 2-week incubation period, cell growth with gradual erosion and cracking was observed on the surface of the PLA matrix [Fig. 7(B)]. After 6 weeks, the disruption of the PLA matrix became more obvious [Fig. 7(C)]. This degradation was confirmed by increasing weight loss of the PLA matrix as a function of incubation time (Fig. 8), which reached nearly 10% after only 14 weeks. The most likely cause of this weight loss was biodegradation.

The SEM photomicrographs in Figure 7 indicate that the PLA-*g*-AA/SF (20 wt %) composites were more readily degraded than neat PLA. After a 2-week incubation period, the PLA-*g*-AA/SF composite was coated with a biofilm of bacterial cells [Fig. 7(J)], indicating more cell growth than that observed on PLA at the same incubation time. Moreover, at 6 and 14 weeks, larger pores were apparent in the PLA-*g*-AA/SF composite [Fig. 7(K,L)], indicating a higher level of degradation. The rate of weight loss of the PLA-*g*-AA/SF composites was also accelerated relative to that of PLA, exceeding 25% after 14 weeks (Fig. 8). These results demonstrate that the addition of SF to the AA-grafted PLA enhanced the biodegradability of the composite.

Figure 8 shows the percent weight change as a function of time for PLA/SF and PLA-*g*-AA/SF composites buried in the soil compost. For both composites, the degree of weight loss increased with SF content. Composites with 40 wt % SF degraded rapidly over the first 6 weeks, losing a mass equivalent to their approximate SF content, and showed a gradual decrease in weight over the next 6 weeks. PLA-*g*-AA/SF exhibited a weight loss of ~ 2–8 wt %.

CONCLUSIONS

The compatibility and mechanical properties of SF blended with PLA and AA-modified PLA (PLA-*g*-AA) were examined. FTIR and NMR analyses revealed the formation of ester groups from reactions between —OH groups in SF and carboxyl groups in PLA-*g*-AA, significantly altering the structure of the composite material. Although DSC curves indicated a decrease in melting temperature for both PLA/SF and PLA-*g*-AA/SF with increasing SF content, the PLA-*g*-AA/SF composites were more easily processed because of both lower melt temperatures and lower mixing torques. The glass transition temperature of PLA-*g*-AA/SF was higher than that of PLA/SF, indicating a more hindered molecular motion.

The morphology of the PLA-*g*-AA/SF composites was consistent with good adhesion between the SF phase and the PLA-*g*-AA matrix. In mechanical tests, AA grafting enhanced the mechanical properties of the composite, especially the tensile strength. Although the water resistance of PLA-*g*-AA/SF was higher than that of PLA/SF, the biodegradation rate of PLA-*g*-AA/SF was lower than that of PLA/SF, but still higher than that of pure PLA, when incubated in soil. After 14 weeks, the PLA-*g*-AA/SF (40 wt %) composite suffered greater than 60% weight loss. The degree of biodegradation increased with increasing SF content.

References

1. Vinka, E. T. H.; Ra'bagob, K. R.; Glassnerb, D. A.; Gruberb, P. R. Polym Degrad Stab 2003, 80, 403.
2. Wang, K.-H.; Wu, T.-M.; Shih, Y.-F.; Huang, C.-M. Polym Eng Sci 2008, 48, 1833.
3. Graupner, N.; Herrmann, A. S.; Mussig, J. Composites: Part A 2009, 40, 810.
4. Guana, J.; Eskridgeb, K. M.; Hannaa, M. A. Ind Crop Prod 2005, 22, 109.
5. Glenn, G.; Klamczynski, A.; Ludvik, C.; Chiou, B.-S.; Imam, S.; Shey, J.; Orts, W.; Wood, D. Technol Sci 2007, 20, 77.
6. Oksmana, K.; Skrifvarsb, M.; Selinc, J.-F. Comp Sci Tech 2003, 63, 1317.
7. Nampoothiri, K. M.; Nair, N. R.; John, R. P. Bioresour Technol 2010, 101, 8493.
8. Zhang, J.-F.; Sun, X. Macromol Biosci 2004, 4, 1053.
9. Coulembiera, O.; Dege'ee, P.; Hedrickb, J. L.; Dubois, P. Prog Polym Sci 2006, 31, 723.
10. Liang, D.; Hsiao, B. S.; Chu, B. Adv Drug Delivery Rev 2007, 59, 1392.
11. Placketta, D.; Andersenb, T. L.; Pedersenc, W. B.; Nielsenc, L. Comp Sci Tech 2003, 63, 1287.
12. Muller, R. J.; Kleeberg, I.; Deckwer, W. D. J Biotechnol 2001, 86, 87.

13. Wu, C. S. J Appl Polym Sci 2010, 115, 948.
14. Alvarez, V. A.; Ruseckaite, R. A.; Va'zquez, A. Polym Degrad Stab 2006, 91, 3156.
15. Wang, N.; Yu, J.; Ma, X. Polym Int 2007, 56, 1440.
16. Wu, C. S. Macromol Biosci 2005, 5, 352.
17. Shah, B. L.; Selke, S. E.; Walters, M. B.; Heiden, P. A. Polym Comp 2008, 29, 655.
18. Breitenbach, A.; Li, Y. X.; Kissel, T. J Contr Release 2000, 64, 167.
19. Martins, M. A.; Forato, L. A.; Mattoso, L. H. C.; Colnago, L. A. Carbohydr Polym 2006, 64, 127.
20. Wu, C. S. J Appl Polym Sci 2004, 94, 1000.
21. Wang, K.-H.; Wu, T.-M.; Shih, Y.-F.; Huang, C.-M. Polym Eng Sci 2008, 48, 1833.
22. Prinos, J.; Bikiaris, D.; Theologidis, S.; Panayioyou, C. Polym Eng Sci 1998, 38, 954.
23. Raquez, J. M.; Nabar, Y.; Narayan, R.; Dubois, P. Macromol Mater Eng 2008, 293, 310.